Journal of Physics: Conference Series **656** (2015) 012164 doi:10.1088/1742-6596/656/1/012164

Ventilated cavity flow over a backward-facing step

B W Pearce[1], P A Brandner[1], S J Foster[2]

[1] Australian Maritime College, University of Tasmania, Launceston, Tasmania 7250, Australia
[2] Incat Crowther, Sydney, NSW 2084, Australia

E-mail: Bryce.Pearce@utas.edu.au

Abstract. Ventilated cavities detaching from a backward facing step (BFS) are investigated for a range of upstream boundary layer thicknesses in a cavitation tunnel. The upstream turbulent boundary layer thickness is varied by artificial thickening of the test section natural boundary layer using an array of transversely injected jets. Momentum thickness Reynolds numbers from 6.6 to 44×10^3 were tested giving boundary layer thickness to step height ratios from 1.25 to 3.8. A range of cavity lengths were obtained by variation of the ventilation flow rate for several freestream Reynolds numbers. Cavity length to step height ratios from 20 to 80 were achieved. Cavity length was found to be linearly dependent on ventilation rate and to decrease with increasing boundary layer thickness and/or Reynolds number. This result may have implications in the practical optimization of these flows which occur in applications such as drag reduction on marine hull forms.

1. Introduction

A significant portion of the propulsive power requirements for a marine vessel, up to around 60%, is required to overcome the frictional drag due to the wetted surface area. For displacement hull forms there has been recent interest in the modification of the near-hull flow field, e.g. by the addition of air bubbles/air layer [1, 2] or polymer solutions [3, 4], to reduce viscous hull resistance. A subset within the broader air bubble/air layer drag reduction field is the formation of air filled cavities from backward-facing steps (BFS) in the hull. Developmental trials and basic studies have used air cavities covering 30 to 50% of the wetted hull surface [5, 6]. An aspect of these BFS cavity flows which has not been considered in previous studies is the effect of the upstream turbulent boundary layer on the cavity physics. If significant, it may influence the efficiency of the drag reduction system and inform the optimal longitudinal location of the BFS, which determines the boundary layer thickness of the flow at the point of cavity detachment. The present work reports on aspects of an experimental investigation on the effect that an upstream boundary layer has on the geometry of a ventilated cavity forming from a BFS. A sketch of the basic flow investigated is shown in Figure 1.

2. Experimental Overview

Experiments were carried out in the Cavitation Research Laboratory (CRL) water tunnel at the University of Tasmania. The tunnel test section is 0.6 m square by 2.6 m long and has operating velocity and pressure ranges of 2 to 12 m/s and 4 to 400 kPa absolute respectively. The CRL water tunnel was developed with a capability to artificially thicken (or thin) the test section ceiling boundary layer to range from nominally 0.01 to 0.1 m thick within the test section

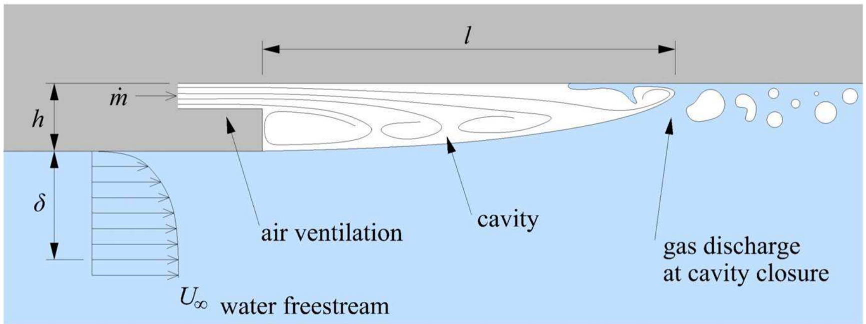

Figure 1: Sketch of a ventilated cavity detaching from a BFS with relevant flow features and parameters noted.

length. These thickened boundary layer profiles being close approximations to flat plate, zero pressure gradient, high Reynolds number turbulent boundary layers [7]. The tunnel also has ancillary systems for rapid degassing and for continuous injection and removal of nuclei and large volumes of incondensable gas. A detailed description of the facility is given in [8, 9] and detailed specifications for the associated instrumentation can be found in [10].

A 2-D plate (750 mm × 10 mm) with a 'quarter' ellipse (5:1) leading edge was attached to the test section ceiling. Compressed air is supplied through the tunnel wall into an internal manifold within the rear section of the plate from which air is admitted into the separation zone downstream of the BFS via an array of nozzles. The boundary layer profiles were measured on the test section vertical center plane, 50 mm upstream from the end of the plate, using a total head tube [11] . Images of the cavity were taken from below using a Canon EOS 50D SLR camera with a Canon EF24-70 mm zoom lens.

All tests, including boundary layer measurements, were conducted at constant Reynolds numbers (Re), based on test section height , of $3, 4$ & 5×10^6 (corresponding to step height based Reynolds numbers of $50, 66.7$ & 83.3×10^3). For the ventilated cavity measurements, the freestream cavitation number (i.e. that based on the liquid vapor pressure), σ_v, was kept at a constant value of 1.2. $\sigma_v = (p_\infty - p_v)/0.5\rho U_\infty^2$ where, p_v is the liquid vapour pressure, p_∞ the freestream reference static pressure, U_∞ is the freestream reference velocity and ρ is the liquid density. A cavitation number based on cavity pressure (with the cavity pressure, p_c exchanged for the p_v in the preceding equation) is also relevant here as the cavity is a mixture of both vapour and incondensable gas, and is denoted as σ_c. The data is presented in terms of an air entrainment coefficient, $C_Q = (\dot{m}/\rho_a)/(hwU_\infty)$, where ρ_a is the air density, $\dot{m}$ is the mass flow rate into the cavity and h and w are the height and width of the step.

3. Results and Discussion

As the cavity closure is inherently unsteady, a mean cavity length was determined for each flow condition from the average of ten images with the closure oscillating typically over a length of 5 to 10% [11]. Typical images of the ventilated cavity are shown in figure 2. From the initial detachment from the step, the cavity surface has a wavy appearance attributable to the turbulence in the upstream boundary layer, with the amplitude of the disturbance growing with downstream distance, eventually contributing to the break up of the cavity. The is due to the mixing of the larger scale structures across the remnant, now decaying, boundary layer. From a previous study on base-ventilated hydrofoils [10, 12], for some conditions the cavity surface was initially undisturbed (glassy appearance) attributable to a laminar boundary layer upstream of the step. Figure 2 (a) and (c) show the increase in cavity length with a reduction in boundary layer thickness for constant Re and similar C_Q. This is attributable the decrease in the mean kinetic energy in the overlying inter-facial layer. Similarly (b) and (d) show the decrease in cavity length with increase in Re due to the greater turbulent kinetic energy in this case. With an increase in Re it is observed that greater breakup occurs along the cavity surface indicating

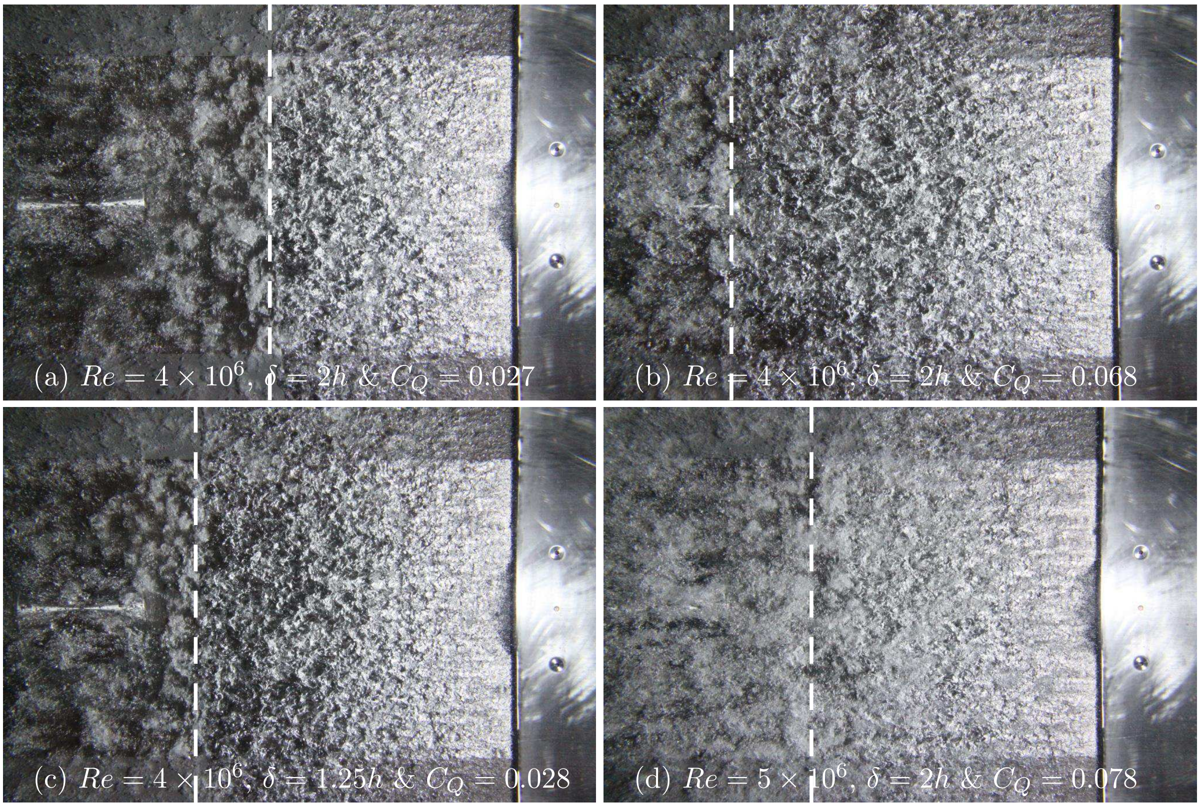

Figure 2: Typical images of the ventilated cavity detaching from a BFS for $Re = 4$ & 5×10^6 and $\delta/h = 1.25$ & 2.0. The 2-D nature of the cavity is apparent indicating that the ventilation flow is sufficiently distributed across the span of the step. The cavity closure is identifiable (indicated by the white dashed line) with air discharging from the closure region in shed cloud cavities and individual bubbles. Flow is from right to left.

that additional air entrainment is occurring along the interface (also observed by Arndt et.al. [13]), which would contribute to a reduced cavity length.

The effect of ventilation rate, boundary layer thickness and Reynolds number on cavity length is shown in figure 3. Cavity length increases linearly with ventilation rate (see also figure 2 (a) and (b)) and reduces with increase in boundary layer thickness and/or Reynolds number. The latter effect is due to the reduced 'local' freestream velocity at the step outer edge due to the presence of the boundary layer. This consequently reduces the denominator in σ_c resulting in an effectively lower cavitation number which implies a shorter cavity length. As discussed above, the reduced cavity length with increase in Re may be attributable to the increase in air loss through the cavity surface. There is a difference in slope between the thinned and/or natural boundary layers ($\delta = 1.25h$ & $2h$) and the two thickened boundary layers for the lower Reynolds number data which may be attributable to a difference in turbulence profiles as the mean velocity profiles, except for the thickest boundary layer, are virtually identical [7, 11]. Turbulence profile measurements are planned, but have not been made for the present study.

As described in [12] the cavitation number was experimentally measured and found to be very small, $\sigma_c \ll 0.1$ which is expected for this flow geometry. The results presented here have not included σ_c as there was a large scatter in the measurements due to the technique used discussed in more detail in the earlier publication [12].

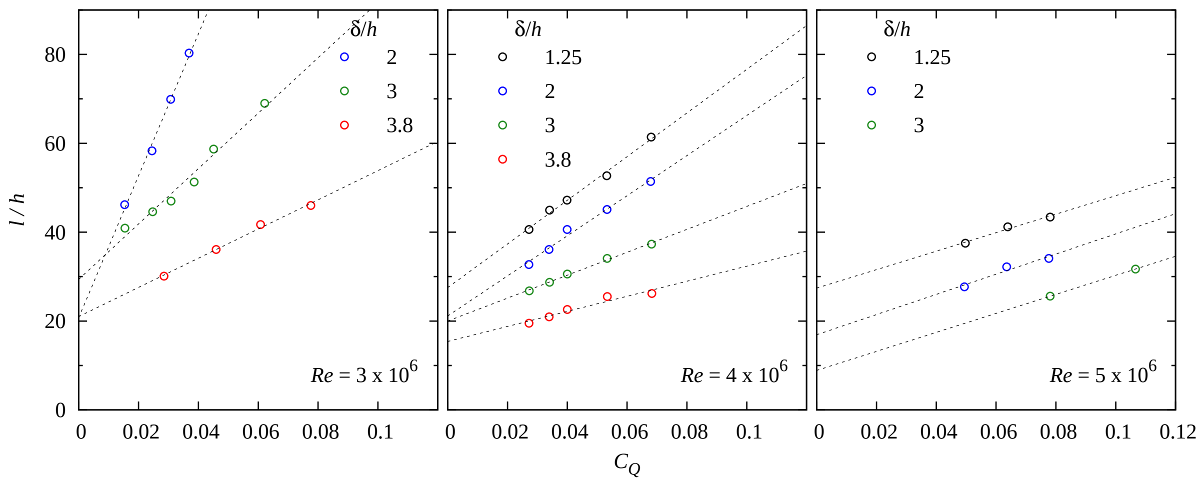

Figure 3: Cavity length versus ventilation rate for the four boundary layer thicknesses and three Reynolds numbers tested. The straight lines are linear least square fits through the experimental data indicating that the cavity length is linearly dependent on the ventilation rate.

4. Conclusions

The ventilated cavity flow over a BFS has been experimentally investigated as to the dependence of the cavity geometry on the Reynolds number, ventilation rate and upstream boundary layer thickness. The cavity length was found to increase linearly with ventilation rate and decreases with both increased boundary layer thickness and/or Reynolds number. This dependence of the cavity geometry on the upstream boundary layer thickness has implications for the longitudinal location of the BFS on a vessel hull employing such a device for viscous drag reduction.

Acknowledgments

The authors wish to acknowledge the assistance of Mr Robert Wrigley in carrying out the experiments and the support of the Australian Maritime College.

References

[1] Ceccio S L 2010 *Ann. Rev. Fluid Mech.* **42** 183–203
[2] Elbing B R, Mkiharju S, Wiggins A, Perlin M, Dowling D R and Ceccio S L 2013 *J. Fluid Mech.* **717** 484–513
[3] Procaccia I, Lvov V S and Benzi R 2008 *Rev. Mod. Physics* **80** 225–247
[4] Elbing B R, Dowling D R, Perlin M and Ceccio S L 2010 *Phys. Fluids* **22** 045102
[5] Lay K A, Yakushiji R, Mkiharju S, Perlin M and Ceccio S L 2010 *J. Ship Res.* **54** 109–119
[6] Shiri A, Leer-Andersen M, Bensow R E and Norrby J 2012 *29th Symposium on Naval Hydrodynamics* (Gothenburg, Sweden: ONR)
[7] Brandner P A, Belle A, Pearce B W and Holmes M J 2012 *18th Australasian Fluid Mechanics Conference* (Launceston, Australia: AFMS) paper 228
[8] Brandner P A, Lecoffre Y and Walker G J 2007 *16th Australasian Fluid Mechanics Conference* (Gold Coast, Australia: School of Engineering, University of Queensland) pp 630–637
[9] Brandner P A, Lecoffre Y and Walker G J 2006 *Sixth International Symposium on Cavitation - CAV2006* (Wageningen, The Netherlands: MARIN)
[10] Pearce B W and Brandner P A 2012 *Eighth International Symposium on Cavitation - Cav2012* (Singapore: Research Publishing) paper 218
[11] Pearce B W, Brandner P A, Foster S and Zarruk G A 2014 *19th Australasian Fluid Mechanics Conference* (Melbourne, Australia: RMIT University) paper 129
[12] Pearce B and Brandner P 2012 *18th Australasian Fluid Mechanics Conference* (Launceston, Australia: AFMS) paper 391
[13] Arndt R E A, Hambleton W T, Kawakami E and Amromin E L 2009 *J. Fluids Eng.* **131** 111301